Mathematical Biosciences and Engineering

MBE, 16(6): 7217–7229.
DOI: 10.3934/mbe.2019362
Received: 25 March 2019
Accepted: 28 July 2019
Published: 08 August 2019

http://www.aimspress.com/journal/MBE

*Research article*

# Exome sequencing identifies predisposing and fusion gene in ganglioneuroma, ganglioneuroblastoma and neuroblastoma

**Wei Wu, Weijue Xu, Jiangbin Liu, Jun Sun, Yimin Huang and Zhibao Lv***

Department of General Surgery, Children's Hospital of Shanghai, Shanghai Jiao Tong University, Shanghai 200030, China

*** Correspondence:** Email: lvzhibao@sohu.com; Tel: +86-021-62474880; Fax: +86-021-62474880.

**Abstract:** This study intended to gain new insight into the genetic basis underlying ganglioneuroma (GN), ganglioneuroblastoma (GNB), and neuroblastoma (NB). Three fresh-frozen surgically resected tumor tissues (GN1, GNB1, and NB1) and matched blood samples (GN2, GNB2, and NB2) were respectively obtained from three pediatric patients with GN, GNB, and NB. After exome sequencing, we predicted the somatic single nucleotide variants (SNV) and insertion and deletion (InDel), and screened the predisposing genes. Finally, we detected and filtered the fusion gene using Fusionmap. Exome sequencing identified 815, 985, and 884 somatic SNV, and 56, 43, and 34 InDel for GN, NB, and GNB respectively. Total 29, 19 and 37 predisposing genes were identified from GN, GNB and NB samples, such as *PIK3CA* (GN), *MUC4* (GN), *PML* (NB), *TFR2* (GNB), and *MAX* (GNB). Additionally, four common fusion genes, such as *HOXD11-AGAP3* and *SAMD1-CDC42EP5*, were identified from three tumor samples. Moreover, *SAMD1-CDC42EP5* was also a common fusion position in three blood samples. These previously unrecognized predisposing genes, such as *PIK3CA*, *MUC4*, *PML*, *TFR2* and *MAX*, and fusion genes, like *HOXD11-AGAP3*, and *SAMD1-CDC42EP5* may have the potential to impact the progression and development of neuroblastic tumors.

**Keywords:** ganglioneuroma; ganglioneuroblastoma; neuroblastoma; exome sequencing; predisposing gene

## Abbreviations

GN: ganglioneuroma; GNB: ganglioneuroblastoma; NB: neuroblastoma; ALK: anaplastic lymphoma kinase; MYCN: myelocytomatosis viral oncogene neuroblastoma derived homolog; SNV:

single nucleotide variants; InDel: insertion and deletion.

## 1. Introduction

Ganglioneuroma (GN), ganglioneuroblastoma (GNB), and neuroblastoma (NB) are tumors of sympathetic nervous system derived from primitive sympathogonia, which are referred to collectively as neuroblastic tumors [1]. GN is the most benign form, composing of ganglion cells and mature neuromatous stroma. GNB consists of both immature ganglion cells and differentiating neuroblasts, which indicates potentially malignant behavior. NB is the most immature, undifferentiated, and malignant form, showing spontaneous or induced differentiation to GNB or GN [2]. Specially, the neuroblastic tumors mainly occur in children, among which, NB is one of the most common pediatric malignancy, accounting for 10% of pediatric cancers [3]. Presently, surgery and chemotherapy are main therapeutic approaches. Despite recent advances in treatment, NB remains a relatively lethal tumor, accounting for 15% of childhood cancer fatalities [4]. It has been reported that tumorigenesis is a consequence of a loss of functions in some critical genes [5], which leads to the proposal that exploring the predisposition genes may help to early diagnosis and treatment of these tumors.

Like other solid tumors, neuroblastic tumors are also thought to initiate and progress through a series of genetic alterations [6]. For instance, many familial neuroblastic tumors are explained by anaplastic lymphoma kinase (ALK) or paired like homeobox 2b (PHOX2B) mutations [7]. Additionally, mutations in v-Myc avian myelocytomatosis viral oncogene neuroblastoma derived homolog (MYCN), and cyclin D2 (CCND2) are often found in NB [8]. WAS protein family member 3 (WAVE3) is truncated and inactivated as a result of a chromosome translocation in GNB [9]. In spite of these findings, considerable information about the contribution of somatic point mutations to the pathogenesis of neuroblastic tumors remains largely unknown.

Recently, the development of next-generation sequencing technologies make it feasible to reveal extensive potential cancer-driving genes in human cancers [10,11]. Several genome studies of solid tumors concentrate analysis on exome to increase the possibility of identification of driver mutations [12,13]. To further gain more knowledge about the genetic basis underlying the three types of neuroblastic tumors, we performed exome sequencing for targeted exon capture in three pediatric patients with GN, GNB, and NB. Based on the sequence data, we predicted the somatic single nucleotide variants (SNV) and insertion and deletion (InDel). It has been reported that fusion genes are related to some cancer types. Cell lines that carry translocations are important models for the study of oncogenic properties of fusion proteins, which may contribute to develop therapeutic strategies. Therefore, we screened the predisposing genes and fusion genes of the tumors.

## 2. Materials and method

### *2.1. Samples collection*

Three pairs of fresh-frozen surgically resected tumor tissues (GN1, GNB1, and NB1) and matched blood samples (GN2, GNB2, and NB2) were respectively obtained from three pediatric patients (age range 4–5 years) with GN, GNB, and NB in Children's Hospital of Shanghai between July and August in 2016. All patients had given their informed consent, and this study was approved

by the local Research Ethics Committee. This study was conducted on September 20th, 2016.

### *2.2. Genomic DNA libraries preparation and sequencing*

DNA was isolated from samples using the QIAGEN DNeasy Tissue kit (Qiagen, USA) according to the protocol. After detection of the purity and concentration of DNA, genomic DNA libraries were prepared. Briefly, genomic DNA was fragmented and adaptors were ligated to the fragments. The adaptor-ligated templates were fractionated using agarose gel electrophoresis and the fragments of the desired size were excised. Genomic DNA libraries were hybridized to biotin labeled RNA probes with Agilent SureSelect capture array (Agilent, USA) to capture targeted genomic sequences and the unbound genomic DNA was eluted. After PCR amplification, the purity and concentration of libraries were detected and the qualified libraries were sequenced on the Illumina HiSeq platform.

### *2.3. Sequence data processing and quality control*

Exome sequence data were processed by removing the adaptor sequences, low-quality reads, and reads with N more than 5%. The obtained clean reads were then mapped to the hg19 human genome by using Burrows-Wheeler-Alignment (BWA) software [14], generating a BAM file. The BAM was ranked with Samtools [15] and the duplication reads were marked with Picard (http://broadinstitute.github.io/picard/).

### *2.4. Somatic mutation detection and annotation*

The SNV and InDel in the exon of target genes were predicted by Samtools mpileup (http://samtools.sourceforge.net) [15] and Varscan2.2.5 [16] based on the matched tumor and blood samples. Then we used SnpEff 4.3 to annotate the obtained SNV and InDel.

### *2.5. Predisposing gene screening*

Predisposing genes refer to genes that can encode genetic diseases or acquire susceptibility to disease under appropriate environmental stimuli. Based on the obtained somatic mutation SNV, we selected the possible predisposing genes through 1000 genome, hapmap, Mills and 1000G, and dbSNP 138 databases. The screening processes were shown as follows: (1) the mutation sites in1000 genome, hapmap, Mills and 1000G, and dbSNP 138 databases were filtered out; (2) the synonymous mutation sites were filtered out; (4) the genes with impact of LOW were filtered out (p-value was set as 0.01).

### *2.6. Functional enrichment analysis of predisposing genes*

The predisposing genes were performed Gene Ontology (GO) function and Kyoto Encyclopedia of Genes and Genomes (KEGG) pathway enrichment analyses using Database for Annotation, Visualization, and Integrated Discovery (DAVID; https://david. ncifcrf.gov). GO includes three categories, biological process (BP), molecular function (MF) and cellular component (CC). Kyoto Encyclopedia of Genes and Genomes (KEGG) and Panther (http.//www.pantherdb.org/) pathway

analyses were used to classify genomic and gene functional information. The significant enrichment results were obtained with p values <0.05.

### *2.7. Fusion gene detection*

Fusionmap (http://www.omicsoft.com/fusionmap) [17] provides an systematic and accurate solution to detect fusion events through junction-spanning reads. In this study, Fusionmap was used to detect and filter the somatic fusion gene.

## 3. Results

### *3.1. Sequence data preprocessing*

After mapping the clean reads to hg19 human genome, the obtained map rate was more than 99%, fraction of target covered ≥ 40X was more than 95%, and coverage of exon was more than 97%. The result of reference genome mapping is shown in Table S1.

**Table S1.** Result of reference genome mapping.

| Sample | GNB1 | NB1 | GN1 | GNB2 | NB2 | GN2 |
|---|---|---|---|---|---|---|
| Read Length (bp) | 150 | 150 | 150 | 150 | 150 | 150 |
| Raw Reads | 151,020,276 | 158,258,214 | 157,718,382 | 41,423,342 | 38,803,050 | 35,842,202 |
| Raw Bases | 22,653,041,400 | 23,738,732,100 | 23,657,757,300 | 6,213,501,300 | 5,820,457,500 | 5,376,330,300 |
| Clean Reads | 142,459,046 | 150,727,394 | 149,668,038 | 39,159,948 | 36,934,792 | 33,789,208 |
| Clean Reads Rate (%) | 94.33 | 95.24 | 94.9 | 94.54 | 95.19 | 94.27 |
| Clean Bases | 21,368,856,900 | 22,609,109,100 | 22,450,205,700 | 5,873,992,200 | 5,540,218,800 | 5,068,381,200 |
| Low-quality Reads | 2,112,918 | 1,555,196 | 1,628,694 | 344,562 | 339,710 | 314,668 |
| Low-quality Reads Rate (%) | 1.4 | 0.98 | 1.03 | 0.83 | 0.88 | 0.88 |
| Ns Reads | 9,750 | 32,714 | 10,476 | 2,714 | 8,118 | 2,476 |
| Ns Reads Rate (%) | 0.01 | 0.02 | 0.01 | 0.01 | 0.02 | 0.01 |
| Adapter Polluted Reads | 6,438,562 | 5,942,910 | 6,411,174 | 1,916,118 | 1,520,430 | 1,735,850 |
| Adapter Polluted Reads Rate (%) | 4.26 | 3.76 | 4.06 | 4.63 | 3.92 | 4.84 |
| Raw Q30 Bases Rate (%) | 92.04 | 90.06 | 93.19 | 93.67 | 90.62 | 93.44 |
| Clean Q30 Bases Rate (%) | 92.6 | 90.4 | 93.61 | 93.99 | 90.93 | 93.77 |

Raw Reads: the number of original Reads; Raw Bases (bp): number of original Bases; Clean Reads: number of high quality's Reads after filtration; Clean Reads Rate (%): percentage of Clean Reads in Raw Reads; Clean Bases (bp): number of high quality's Bases after filtration; Low-quality Reads: number of removed low quality Reads; Low quality Reads Rate (%): percentage of removed low quality Reads in Raw Reads; Ns Reads: removed Reads with N more than 5%; Ns Reads Rate (%): percentage of removed Ns Reads in Raw Reads; percentage of removed: number of removed adapter polluted Reads; Adapter Polluted Reads Rate (%): percentage of removed adapter polluted Reads in Raw Reads; Raw Q30 Bases Rate (%): percentage of Bases with sequencing quality value more than 30 (error rate less than 0.1%) of Raw Reads in Raw Bases; Clean Q30 Bases Rate (%): percentage of Bases with sequencing quality value more than 30 (error rate less than 0.1%) of Clean Reads in Clean Bases.

*3.2. Somatic SNV and InDel detection and annotation*

The total numbers of somatic SNV in three pairs of samples (tumor matched with blood) were 815, 985, and 884 for GN, NB, and GNB respectively (Figure 1A). Additionally, somatic InDel in three pairs of samples were 56, 43, and 34, respectively (Figure 1B).

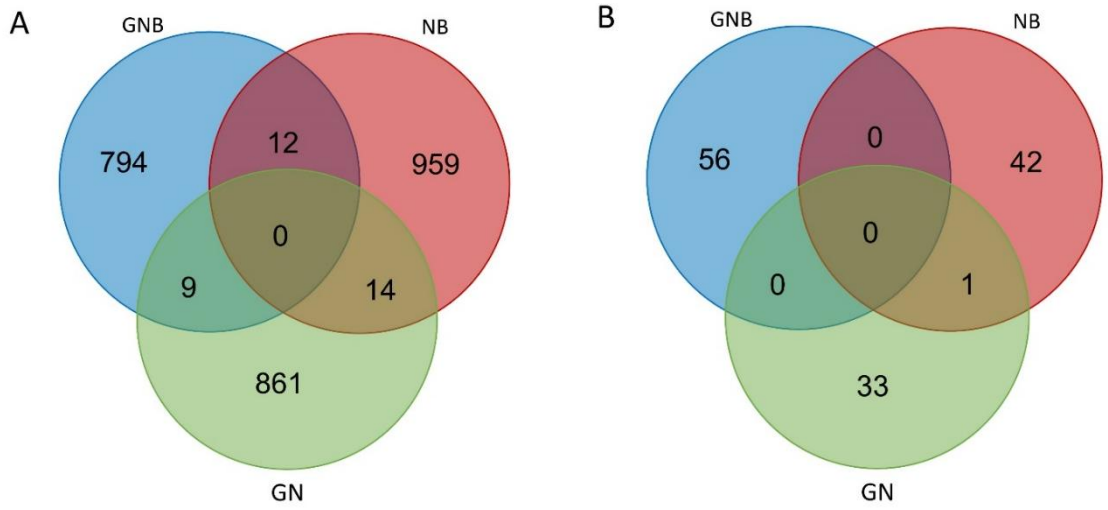


**Figure 1.** The total numbers of somatic (A) SNV and (B) InDel in three pairs of samples (tumor matched with blood).

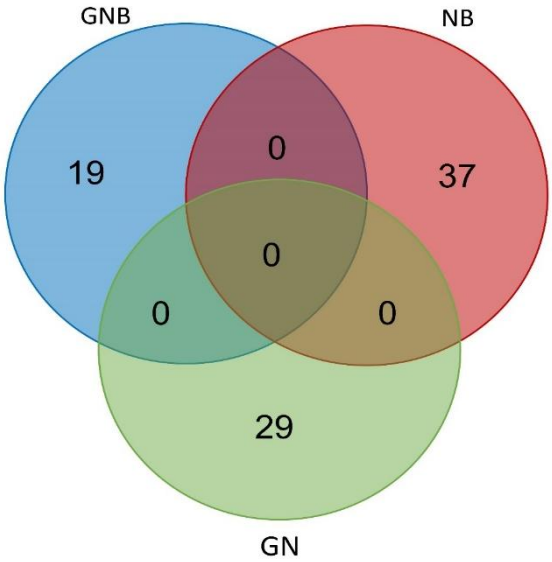


**Figure 2.** The total numbers of predisposing genes identified from ganglioneuroblastoma (GNB), neuroblastoma (NB), and ganglioneuroma (GN) samples.

*3.3. Predisposing gene screening*

A total of 29, 19 and 37 predisposing genes were identified from GN, GNB and NB samples, as

shown in Figure 2. The top ten predisposing genes (with low p-values) for the three types of neuroblastic tumors are show in Table 1, such as phosphatidylinositol-4,5-bisphosphate 3-kinase catalytic subunit alpha (PIK3CA; GN), mucin 4, cell surface associated (MUC4; GN), promyelocytic leukemia (PML; NB), olfactory receptor family 4 subfamily F member 4 (OR4F4; GNB), transferrin receptor 2 (TFR2; GNB), and MYC associated factor X (MAX; GNB). Among them, two variations were identified in MUC4, TFR2 and MAX.

**Table 1.** The top ten predisposing genes (with low p-values) for Ganglioneuroma (GN), ganglioneuroblastoma (GNB), and neuroblastoma (NB).

| Sample | Gene name | Chrom | Position | REF | ALT | Mutation type | HGVS.cds | HGVS.protein | Ref reads count in blood | Mutated reads count in blood | Ref reads count in blood tumor | Mutated reads count in tumor |
|---|---|---|---|---|---|---|---|---|---|---|---|---|
| GN | PIK3CA | chr3 | 178952085 | A | G | structural interaction | c.3140A>G | | 62 | 0 | 161 | 86 |
| GN | ITIH6 | chrX | 54780171 | G | A | stop gained | c.3265C>T | p. Gln1089* | 42 | 0 | 100 | 59 |
| GN | SHROOM2 | chrX | 9859078 | C | T | missense | c.379C>T | p. Pro127Ser | 64 | 0 | 109 | 50 |
| GN | XK | chrX | 37587287 | G | T | missense | c.907G>T | p. Asp303Tyr | 53 | 0 | 199 | 89 |
| GN | VCAN | chr5 | 82835573 | C | A | missense | c.6751C>A | p. Leu2251Ile | 41 | 0 | 149 | 71 |
| GN | MUC4 | chr3 | 195510454 | G | T | missense | c.7997C>A | p. Ser2666Tyr | 71 | 1 | 201 | 32 |
| GN | MUC4 | chr3 | 195510470 | T | C | missense | c.7981A>G | p. Ser2661Gly | 59 | 3 | 186 | 45 |
| GN | NPIPB11 | chr16 | 29395259 | C | G | missense | c.994G>C | p. Ala332Pro | 95 | 2 | 306 | 42 |
| GN | USP17L25 | chr4 | 9351547 | C | T | missense | c.929C>T | p. Pro310Leu | 149 | 7 | 554 | 79 |
| GN | SPDYE2 | chr7 | 102197649 | G | C | missense | c.649G>C | p. Asp217His | 56 | 2 | 173 | 37 |
| NB | EFR3B | chr2 | 25353483 | T | G | missense | c.833T>G | p. Ile278Ser | 96 | 3 | 270 | 54 |
| NB | PML | chr15 | 74287220 | A | C | missense | c.67A>C | p. Met23Leu | 52 | 2 | 147 | 29 |
| NB | PPP1CB | chr2 | 28974848 | A | G | 5 prime UTR | c.-143A>G | | 34 | 1 | 116 | 34 |
| NB | NKX6-1 | chr4 | 85419237 | A | G | missense | c.145T>C | p. Ser49Pro | 49 | 0 | 186 | 29 |
| NB | HRNR | chr1 | 152190257 | A | G | missense | c.3848T>C | p. Val1283Ala | 57 | 1 | 236 | 41 |
| NB | RERE | chr1 | 8415615 | T | G | missense | c.4531A>C | p. Met1511Leu | 46 | 1 | 162 | 36 |
| NB | GOLGA8O | chr15 | 32737690 | G | A | missense | c.1601C>T | p. Ala534Val | 38 | 0 | 188 | 34 |
| NB | TRIOBP | chr22 | 38120437 | G | C | missense | c.1874G>C | p. Arg625Thr | 57 | 0 | 157 | 19 |
| NB | BTBD7 | chr14 | 93712457 | T | G | missense | c.2297A>C | p. His766Pro | 39 | 0 | 187 | 30 |
| NB | DEF8 | chr16 | 90030663 | G | C | missense | c.1271G>C | p. Cys424Ser | 63 | 1 | 177 | 24 |
| GNB | OR4F4 | chr15 | 102462504 | C | T | stop gained | c.759G>A | p. Trp253* | 30 | 1 | 53 | 18 |
| GNB | TFR2 | chr7 | 100225860 | G | C | missense | c.1460C>G | p. Thr487Arg | 91 | 1 | 326 | 37 |
| GNB | TFR2 | chr7 | 100225848 | T | C | missense & splice region | c.1472A>G | p. Glu491Gly | 97 | 3 | 348 | 43 |
| GNB | PPIAL4C | chr1 | 144363680 | G | C | missense | c.492C>G | p. Phe164Leu | 40 | 0 | 163 | 26 |
| GNB | LOR | chr1 | 153233663 | T | G | missense | c.238T>G | p. Cys80Gly | 47 | 0 | 113 | 16 |
| GNB | NBPF20 | chr1 | 144217628 | C | G | missense | c.4135C>G | p. Leu1379Val | 91 | 2 | 330 | 37 |
| GNB | CT47A10 | chrX | 120075275 | G | A | missense | c.344C>T | p. Pro115Leu | 13 | 0 | 34 | 19 |
| GNB | MAX | chr14 | 65472918 | C | T | 3 prime UTR | c.*4G>A | | 44 | 1 | 117 | 34 |
| GNB | MAX | chr14 | 65472920 | G | T | 3 prime UTR | c.*2C>A | | 45 | 1 | 131 | 25 |
| GNB | SAMD4A | chr14 | 55034559 | T | C | 5 prime UTR | c.-76T>C | | 49 | 0 | 113 | 16 |


**Figure 3.** Functional enrichment analyses of predisposing genes in ganglioneuroblastoma (GNB), neuroblastoma (NB), and ganglioneuroma (GN) samples.

### *3.5. Functional enrichment analysis of predisposing genes*

Functional enrichment analyses of predisposing genes identified several GO terms and pathway (Figure 3). For instance, PIK3CA was enriched in GO:0004674 protein serine/threonine kinase activity; MUC4 was enriched in GO:0016266 O-glycan processing; PML was enriched in GO:0030155~regulation of cell adhesion; OR4F4 and TFR2 were enriched in GO:0016021 integral component of membrane; MAX was enriched in GO:0030425 dendrite.

### *3.6. Fusion gene detection*

Total 15, 38 and 20 fusion genes were identified from GNB1, NB1 and GN1, respectively. Additionally, 3, 9 and 4 fusion genes were identified from GNB2, NB2 and GN2, respectively. Specially, these fusion genes had not been reported in previous study. The distribution of fusion genes in genome of six samples is shown in Figure 4. By comparing the gene fusion positions among three tumor samples, we found that there were four common fusion positions in three samples, including sterile alpha motif domain containing 1 (SAMD1)-CDC42 effector protein 5 (CDC42EP5), homeobox D11 (HOXD11)-ArfGAP with GTPase domain, ankyrin repeat and PH domain 3 (AGAP3), adrenoceptor alpha 1A (ADRA1A)-zinc finger protein 248 (ZNF248), and importin 4 (IPO4)-dynein heavy chain domain 1 (DNHD1) (Table 2). Moreover, by comparing the gene fusion positions among three blood samples, one common fusion position (SAMD1-CDC42EP5) identified, which was also identified in tumor samples.

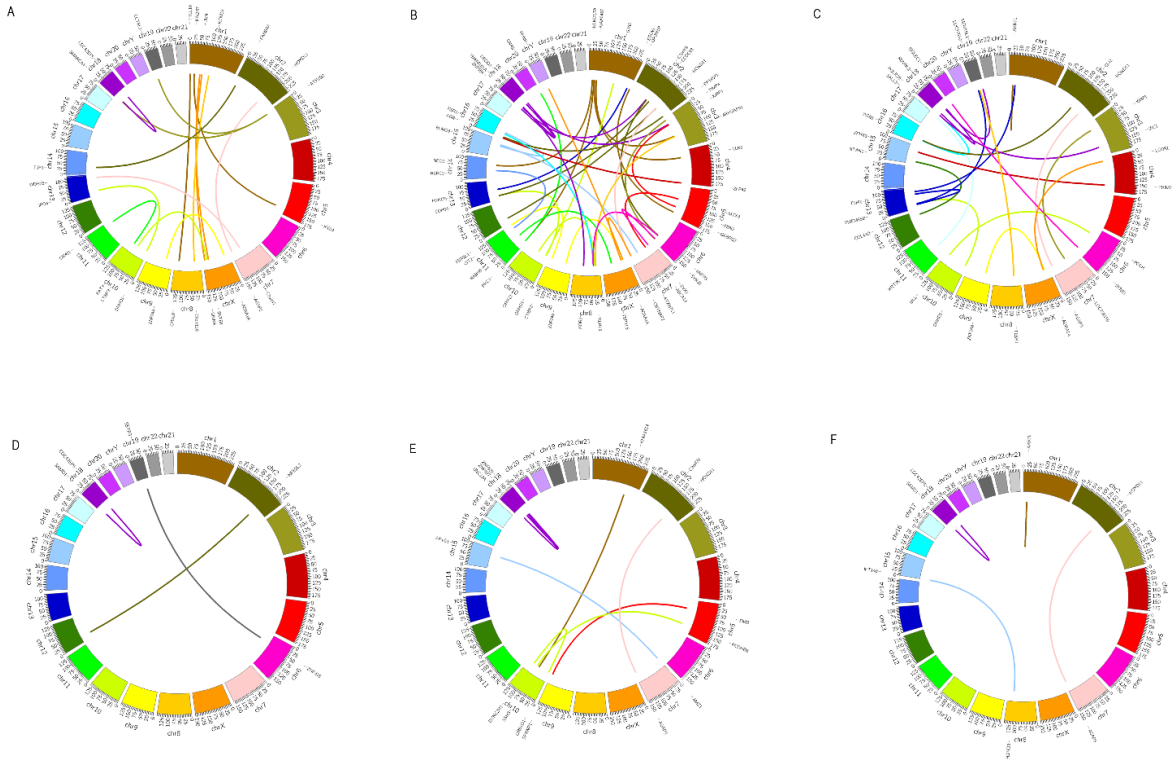


**Figure 4.** The distribution of fusion genes in genome of (A and D) ganglioneuroblastoma (GNB), (B and E) neuroblastoma (NB), and (C and F) ganglioneuroma (GN).

**Table 2.** The common fusion positions in three tumor samples.

| Chr1 | Position1 | Chr2 | Position2 | KnownGene1 | KnownGene2 |
|---|---|---|---|---|---|
| 19 | 14200899 | 19 | 54976551 | SAMD1 | CDC42EP5 |
| 2 | 176972344 | 7 | 150783928 | HOXD11 | AGAP3 |
| 8 | 26623481 | 10 | 38118382 | ADRA1A | ZNF248 |
| 14 | 24650800 | 11 | 6567900 | IPO4 | DNHD1 |

Chr1: the chromosome where the first fusion gene locates; Position1: the fusion position where the first fusion gene locates; Chr2: the chromosome where the second fusion gene locates; Position2: the fusion position where the second fusion gene locates; KnownGene1: the first fusion gene; KnownGene2: the second fusion gene.

## 4. Discussion

In the present study, we performed exome sequencing analysis to identify somatic variation in GN, GNB, and NB. Hundreds of somatic SNVs were identified in three types of tumors. Additionally, dozens of predisposing genes were identified, such as PIK3CA, MUC4 (GN), PML (NB), TFR2 and MAX (GNB). These predisposing genes were enriched in several GO functions. Based on Fusionmap, four common fusion genes, such as HOXD11-AGAP3 and SAMD1-CDC42EP5, were identified from three tumor samples. Moreover, SAMD1-CDC42EP5 was also a common fusion position in three blood samples.

PIK3CA and MUC4 were two predisposing genes in GN. PIK3CA encodes the catalytic subunit p110α of class IA PI3-kinase, which is a member of phosphatidyl-inositol 3-kinases (PI3K) gene family. PI3Ks play an important role in controlling signaling pathways involved in cell proliferation, apoptosis, and invasion [18]. Mutations in genes encoding components of PI3K signaling pathway are common in human cancer [19]. Recent studies have reported a high frequency of somatic missense mutations in PIK3CA of several human cancers [20,21]. MUC4 is a mucin protein, which has anti-adhesive properties contributing to tumor development. MUC4 has been reported to play roles in the progression of cancer [22]. Therefore, we speculated that mutations in PIK3CA and MUC4 may play important roles in the development of GN.

The PML gene negatively regulates survival and proliferation pathways in cancer, which functions as a proapoptotic and growth inhibitory tumor suppressor [23]. In the present study, it was found to be a predisposing gene with somatic missense mutations in NB. Additionally, it was enriched in cell adhesion associated function. Cell-cell adhesion determines the polarity of cells and involves in the maintenance of tissues. Cell-cell adhesiveness is generally declined in human cancers [24]. We speculated that PML mutations may be associated with NB progression by influencing cell adhesion function.

TFR2 is a membrane glycoprotein that mediates cellular iron uptake from holotransferrin. Homozygous mutations of TFR2 cause one form of hereditary hemochromatosis in humans [25]. Specially, TFR2 is found to be frequently expressed in tumor cell lines, such as ovarian cancer, colon cancer and glioblastoma [26]. Its mutations in GNB have not been investigated to our best knowledge. MAX is a constitutively expressed protein, playing a critical role in controlling the MYC/MAX pathway, the deregulation of which contributes to numerous neoplastic conditions [27]. Cominom éndez et al. [28] used exome sequencing suggested that germline-inactivating mutations at MAX was responsible for hereditary pheochromocytoma. In the present study, two 3 prime UTR

variants were found in MAX in GNB, suggesting its potential role in GNB progression.

It has been reported that fusion genes resulting from recurrent chromosomal translocations are related to some cancer types. Cell lines that carry translocations are important models for the study of oncogenic properties of fusion proteins, which may contribute to develop therapeutic strategies [29]. The present study identified four pairs of common fusion genes in three tumor samples. HOXD11 gene is one of the HOX cluster genes, encoding a protein of 338 amino acids with a homeodomain [30]. HOXD11 has been reported to participate in the occurrence of many human malignancies [31,32]. HOXD11 has been found to fused to other gene in acute myeloid leukemia [30]. The present study identified AGAP3 to be a fusion partner of HOXD11. Interestingly, AGAP3 has been reported to be a fusion partner of BRAF in melanoma. Interestingly, HOXD11-AGAP3 has not been reported to involve in the development of neuroblastic tumors. Furthermore, SAMD1-CDC42EP5 was a common fusion position in both tumor and blood samples. SAMD1 is an important transducer of bone morphogenetic protein-2 (BMP-2) and transforming growth factor-β (TGF-β) signals, and has been found to enhance tumor progression [33,34]. Additionally, SAMD1 is involved in the crosstalk between Ras/MEK and BMP/TGF-β pathways, and regulation of these pathways plays a critical role in tumor progression [35,36]. CDC42EP5 is a member of CDC42 effector proteins, acting downstream of CDC42 to induce actin filament assembly leading to cell shape changes [37]. CDC42EP5 was identified to be frequently methylated in ductal carcinoma in situ [38]. Taken together, given the role of HOXD11 and AGAP3, as well as SAMD1 and CDC42EP5 in other tumors, we speculated that HOXD11-AGAP3 and SAMD1-CDC42EP5 fusion expression may play roles in neuroblastic tumors.

Several limitations should be noted in present study. Firstly, the sample size used in this study is limited. The further validation of our findings in a large size sample pool could provide more useful and novel information to understand the mechanisms underlying the progression of these diseases and identify biomarkers for the prognosis. Secondly, despite the present study identified a series of predisposing genes, however, the further validation of them by using clinical samples were still need.

## 5. Conclusion

In conclusion, the present study identified several previously unrecognized predisposing genes, such as PIK3CA, MUC4, PML, TFR2 and MAX, in three kinds of neuroblastic tumors by sequencing the exome. Additionally, HOXD11-AGAP3 and SAMD1-CDC42EP5 fusion expression may play roles in the three types of neuroblastic tumors. These gene coding variants may have the potential to impact tumor behavior, therefore, they may be served as potential targets in the treatments of GN, NB, and GNB. However, the sample size in this study was relatively small, besides, the results were not confirmed by tissue experiments. Therefore, we will continue collecting more samples to validate our findings.

## Acknowledgments

This work was supported by Shanghai Science and Technology Commission (Project number: 12411952405).

## Authors' contributions

Wei Wu and Zhibao Lv did the conception and design. Wei Wu sees to the development of methodology. The sample collection was performed by Weijue Xu, Jiangbin Liu, Jun Sun, Yimin Huang. The analysis and interpretation of data were done by Weijue Xu, Jiangbin Liu. The writing, review, and/or revision of the manuscript were done by Wei Wu, Zhibao Lv, Jiangbin Liu, Jun Sun, and Yimin Huang. All authors read and approved the final manuscript.

## Conflict of interest

The authors have declared that no competing interests exist.

## References


**1.** G. J. Lonergan, C. M. Schwab, E. S. Suarez, et al., From the archives of the AFIP: Neuroblastoma, ganglioneuroblastoma and ganglioneuroma: Radiologic-pathologic correlation 1, *Radiographics*, **22** (2002), 911–934.

2. C. C. Hsiao, C. C. Huang, J. M. Sheen, et al., Differential expression of delta-like gene and protein in neuroblastoma, ganglioneuroblastoma and ganglioneuroma, *Modern pathol.*, **18** (2005), 656–662.

3. J. G. Gurney, R. K. Severson, S. Davis, et al., Incidence of cancer in children in the United States. Sex-, race-, and 1-year age-specific rates by histologic type, *Cancer*, **75** (1995), 2186–2195.

4. J. Brossard, M. L. Bernsteinand and B. Lemieux, Neuroblastoma: an enigmatic disease, *Brit. Med. Bull.*, **52** (1996), 787–801.

5. A. G. Knudson, Mutation and cancer: Statistical study of retinoblastoma, *Proc. Natl. Acad. Sci. USA* **68** (1971), 820–823.

6. H. Carén, F. Abel, P. Kogner, et al., High incidence of DNA mutations and gene amplifications of the ALK gene in advanced sporadic neuroblastoma tumours, *Biochem. J.*, **416** (2008), 153–159.

7. Y. P. Mossé, M. Laudenslager, L. Longo, et al., Identification of ALK as a major familial neuroblastoma predisposition gene, *Nature*, **455** (2008), 930–935.

8. I. Janoueix-Lerosey, D. Lequin, L. Brugières, et al., Somatic and germline activating mutations of the ALK kinase receptor in neuroblastoma, *Nature*, **455** (2008), 967–970.

9. K. Sossey-Alaoui, G. Su, E. Malaj, et al., WAVE3, an actin-polymerization gene, is truncated and inactivated as a result of a constitutional t(1; 13)(q21; q12) chromosome translocation in a patient with ganglioneuroblastoma, *Oncogene*, **21** (2002), 5967.

10. X. Wei, V. Walia, J. C. Lin, et al., Exome sequencing identifies GRIN2A as frequently mutated in melanoma, *Nat. Genet.*, **43** (2011), 442–446.

11. I. Varela, P. Tarpey, K. Raine, et al., Exome sequencing identifies frequent mutation of the SWI/SNF complex gene PBRM1 in renal carcinoma, *Nature*, **469** (2011), 539–542.

12. G. L. Dalgliesh, K. Furge, C. Greenman, et al., Systematic sequencing of renal carcinoma reveals inactivation of histone modifying genes, *Nature*, **463** (2010), 360–363.

13. R. D. Morin, N. A. Johnson, T. M. Severson, et al., Somatic mutations altering EZH2 (Tyr641) in follicular and diffuse large B-cell lymphomas of germinal-center origin, *Nat. Genet.*, **42** (2010), 181–185.

14. H. Liand R. Durbin, Fast and accurate short read alignment with Burrows–Wheeler transform, *Bioinformatics*, **25** (2009), 1754–1760.
15. H. Li, B. Handsaker, A. Wysoker, et al., The sequence alignment/map format and SAMtools, *Bioinformatics*, **25** (2009), 2078–2079.
16. D. C. Koboldt, Q. Zhang, D. E. Larson, et al., VarScan 2: Somatic mutation and copy number alteration discovery in cancer by exome sequencing, *Genome Res.*, **22** (2012), 568–576.
17. H. Ge, K. Liu, T. Juan, et al., FusionMap: Detecting fusion genes from next-generation sequencing data at base-pair resolution, *Bioinformatics*, **27** (2011), 1922–1928.
18. Y. Samuels and V. E. Velculescu, Oncogenic mutations of PIK3CA in human cancers, *Cell Cycle*, **3** (2004), 1221–1224.
19. S. Kang, A. G. Baderand P. K. Vogt, Phosphatidylinositol 3-kinase mutations identified in human cancer are oncogenic, *P. Natl. Acad. Sci. USA*, **102** (2005), 802–807.
20. K. E. Bachman, P. Argani, Y. Samuels, et al., The PIK3CA gene is mutated with high frequency in human breast cancers, *Cancer Biol. Ther.*, **3** (2004), 772–775.
21. Y. Samuels, Z. Wang, A. Bardelli, et al., High frequency mutations of the PIK3CA gene in human cancers, *Science*, **304** (2004), 554.
22. S. K. Srivastava, A. Bhardwaj, S. Singh, et al., MicroRNA-150 directly targets MUC4 and suppresses growth and malignant behavior of pancreatic cancer cells, *Carcinogenesis*, **32** (2011), 1832–1839.
23. R. Bernardi and P. P. Pandolfi, Structure, dynamics and functions of promyelocytic leukaemia nuclear bodies, *Nat. Rev. Mol. Cell Bio.*, **8** (2007), 1006.
24. S. Hirohashi and Y. Kanai, Cell adhesion system and human cancer morphogenesis, *Cancer Sci.*, **94** (2003), 575–581.
25. H. Kawabata, R. E. Fleming, D. Gui, et al., Expression of hepcidin is down-regulated in TfR2 mutant mice manifesting a phenotype of hereditary hemochromatosis, *Blood*, **105** (2005), 376–381.
26. A. Calzolari, I. Oliviero, S. Deaglio, et al., Transferrin receptor 2 is frequently expressed in human cancer cell lines, *Blood Cell Mol. Dis.*, **39** (2007), 82.
27. B. Amati and H. Land, Myc-Max-Mad: A transcription factor network controlling cell cycle progression, differentiation and death, *Curr. Opin. Genet. Dev.*, **4** (1994), 102–108.
28. I. Cominom éndez, F. J. Graciaazn árez, F. Schiavi, et al., Exome sequencing identifies MAX mutations as a cause of hereditary pheochromocytoma, *Nat. Genet.*, **43** (2011), 663.
29. F. Vanoli, M. Tomishima, W. Feng, et al., CRISPR-Cas9-guided oncogenic chromosomal translocations with conditional fusion protein expression in human mesenchymal cells, *P. Natl. Acad. Sci. USA*, (2017).
30. T. Taketani, T. Taki, N. Shibuya, et al., The HOXD11 gene is fused to the NUP98 gene in acute myeloid leukemia with t(2;11)(q31;p15), *Cancer Res.*, **62** (2002), 33.
31. D. J. Sharpe, K. S. Orr, M. Moran, et al., POU2F1 activity regulates HOXD10 and HOXD11 promoting a proliferative and invasive phenotype in head and neck cancer, *Oncotarget*, **5** (2014), 8803–8815.
32. S. Bhatlekar, J. Z. Fieldsand B. M. Boman, HOX genes and their role in the development of human cancers, *J. Mol. Med.*, **92** (2014), 811–823.
33. E. Langenfeld, Y. Kongand J. Langenfeld, Bone morphogenetic protein 2 stimulation of tumor growth involves the activation of Smad-1/5, *Oncogene*, **25** (2006), 685.

34. X. Liu, J. Yue, R. S. Frey, et al., Transforming growth factor β signaling through Smad1 in human breast cancer cells, *Cancer Res.*, **58** (1998), 4752–4757.
35. J. Yue, R. S. Frey and K. M. Mulder, Cross-talk between the Smad1 and Ras/MEK signaling pathways for TGFβ, *Oncogene*, **18** (1999), 2033.
36. M. Kretzschmar, J. Doody and J. Massagu, Opposing BMP and EGF signalling pathways converge on the TGF-β family mediator Smad1, *Nature*, **389** (1997), 618.
37. D. S. Hirsch, D. M. Pirone and P. D. Burbelo, A New Family of Cdc42 Effector Proteins, CEPs, Function in Fibroblast and Epithelial Cell Shape Changes, *J. Biol. Chem.*, **276** (2001), 875–883.
38. M. Hu, J. Yao, L. Cai, et al., Distinct epigenetic changes in the stromal cells of breast cancers, *Nat. Genet.*, **37** (2005), 899–905.


AIMS Press

©2019 the Author(s), licensee AIMS Press. This is an open access article distributed under the terms of the Creative Commons Attribution License (http://creativecommons.org/licenses/by/4.0)